CHEMISTRY OF MATERIALS

COMMUNICATION

pubs.acs.org/cm

Are Zeolite Films Flexible?

Theodoros Baimpos,[†] Dimitris Kouzoudis,[‡] Leszek Gora,[§] and Vladimiros Nikolakis*[,†]

[†]Foundation for Research & Technology Hellas, Institute of Chemical Engineering & High Temperature Chemical Processes, PO Box 1414, 26504, Greece

[‡]Department of Engineering Sciences, University of Patra, Karatheodori Str, 26504, Patras, Greece

[§]Catalysis Engineering-The Pore, DelftChemTech, Delft University of Technology, Julianalaan 136, 2628BL Delft, The Netherlands

Supporting Information

KEYWORDS: porous materials, zeolite membranes, silicalite-1, adsorption induced strain, MFI, zeolite film flexibility

Since the beginning of the 1990's, there has been significant interest in the development of synthesis methods of pinhole free, mechanically stable, polycrystalline-supported zeolite films. Depending on the support and the properties of the zeolite, such films have been studied as membranes for gas separations,[1] sensors,[2] low-k dielectric films,[3] corrosion resistance barriers, antimicrobial coatings,[4] and as hosts of optically or electrically active guest molecules.[5−7]

Silicalite-1 is among the most studied zeolites for the formation of polycrystalline membranes, primarily because of the existence of numerous robust synthesis conditions, as well as its inherent molecular sieving properties. The tremendous advances toward understanding silicalite-1 crystallization, the development of methods for the controlled deposition or self-assembly of crystal monolayers on surfaces,[7] as well as the development of novel organic template removal methods[8,9] made possible the rational design and preparation of silicalite-1 films with controlled orientation, grain boundary size, and number density.[10−12]

Until recently, it was believed that zeolite membranes, in contrast to polymeric materials, do not swell due to adsorption. Nair et al. have indicated that the adsorption of p-xylene in silicalite-1 films might cause deformation of the crystals and grain boundary openings.[13,14] Furthermore, findings by H. Morell et al. show that silicalite-1 crystals which are saturated with n-hexane at 180K, expand considerably.[15] Recently, S.G. Sorenson et al.[16] have shown that the adsorption of n-alkanes (C_4−C_8) and i-butane at room temperature expands the unit cell volume between 0.42 and 1.19%, in contrast to adsorption of benzene that did not result in any detectable unit cell volume changes. Adsorption induced strains on silicalite-1 crystals have been found to significantly affect membrane performance. For example, adsorption induced expansion in silicalite-1 membranes reduced permeation through nonzeolitic pores.[17−20] This effect was so pronounced that in some cases, it significantly enhance permselectivity.[19,21] On the other hand, adsorption of compounds at loadings that shrink the unit cell size of silicalite-1 might have the opposite effect.[22]

Adsorption induced strains also play a major role in the performance of chemical sensors based on zeolite film. We have recently shown that zeolite films grown on the surface of magnetoelastic ribbons can be used as selective sensors for the detection of light gases[23] or light hydrocarbons.[24,25] The resonance frequency of the sensor depends on the reciprocal of the effective density of the sensor, and thus it should drop as the film is loaded with gas. However, in the case of n-hexane detection by a silicalite-1/Metglas sensors (Metglas is a magnetoelastic material) the opposite effect was observed (the resonance frequency increased with n-hexane loading). This increase can be attributed to adsorption-induced stresses which according to the Villari effect in magnetoelastic materials, alter their magnetic state[26,27] and have an additional influence on the measured resonance frequency.

To examine the elasticity and flexibility of the zeolite films due to adsorption induced strains, we initially studied the effect of n-hexane adsorption in silicalite-1 polycrystalline films synthesized on the external surface of 30 μm thick Metglas ribbons. The molar composition of the synthesis sol was: 1.5TPAOH:19.5-SiO_2: 438H_2O.[28,29] Four different films with masses 8.9, 10.9, 12.6, and 19.2 mg were prepared by adjusting the synthesis duration. In order to avoid heating the ribbons above 350 °C (Currie temperature of Metglas), the organic template was removed using ozone detemplation, instead of the commonly used calcination in air.[25] For each mass, the resonance frequency increased when the sensor was equilibrated with ∼800 ppm of n-hexane (P/P_s = 0.006) (see Figures S2 and S3 in the Supporting Information), indicating the presence of adsorption-induced stresses. The more pronounced increase was observed in films with the two highest masses. When the 19.2 mg sensor was equilibrated with P/P_s = 0.666 n-hexane vapors, the adsorption induced stress was so intense that a large bending was observed (Figures 1 a, b). The X-ray diffraction patterns of the two sides of the sensor are characteristic of the silicalite-1 (Figure 2). Indexing of the two patterns revealed that both sides are monoclinic. The relative intesities of the XRD reflections of the convex side are in relative good agreement with those of the powdern pattern indicating no preffered orientation. The XRD pattern of the film crystals on the convex side also do not show any preferred

Received: September 2, 2010
Revised: December 22, 2010
Published: February 22, 2011

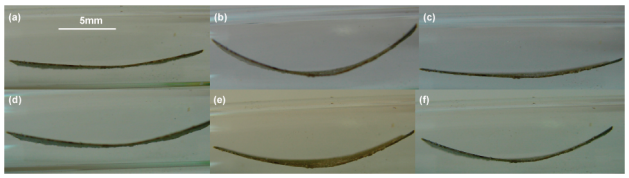

Figure 1. Side view photographs of the silicalite-1 film coated metglas ribbon (a) in air and equilibrated with $P/P_s \sim 0.666$ of (b) *n*-hexane, (c) *c*-hexane, (d) benzene, (e) *o*-xylene, (f) *p*-xylene vapors. The mass of the zeolite film was 19.2 mg and the length of the ribbon is 2 cm.

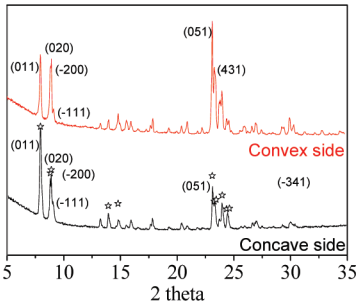

Figure 2. XRD patterns of the two sides of the metglas ribbon after the silicalite-1 film synthesis and ozone treatment (the stars denote the reflections of the calcined silicalite-1 powder pattern;[30] the term convex and concave refers to the bottom and upper side of the ribbon as shown in Figure 1).

orientation. However, the increased relative intensity of the (020), (051), and (431) reflections indicates that a higher number of film crystals has these directions perpendicular to the surface of the ribbon.

When hexane was replaced by air, the ribbon approximately assumed its initial shape. The periodic cycling of high n-hexane concentration ($P/P_s = 0.666$) and air was repeated several times at room temperature and it was video recorded. The shapes in images a and b in Figure 1 reappear in each cycle, even after several adsorption−desorption cycles (see video in Supporting Information). Bending of the ribbon, but to a different extend, was also observed after equilibration with vapors of *c*-hexane, benzene, *o*-xylene, and *p*-xylene (in all cases, $P/P_s = 0.666$).

The data clearly demonstrate that the adsorption of hydrocarbon vapors in silicalite-1 crystals induces nonpermanent strain, which does not destroy the connectivity of the zeolite film, proving that zeolite films can be both flexible and elastic. Furthermore, the pronounced bending indicates the presence of important differences between the silicalite-1 films on each side of the ribbon. Indeed, SEM images (Figure 3) of the two sides of the ribbon, taken after the n-hexane adsorption − desorption cycles, indicate that a continuous polycrystalline silicalite-1 film has been formed only on the convex side of the ribbon (Figure 3c, d). On the concave side of the ribbon (Figure 3a, b) scattered silicalite-1 crystals as well as "islands" of polycrystalline layers were formed. The differences between the two sides can also be seen on the photographs of Figure 3 e, f. Because the synthesis conditions are the same for both sides of the ribbon these differences can be attributed to differences on the properties of each metglas surface. Even though they have the same chemical composition the metglass manufacturing process forms ribbons with one side smooth and shinny and one side rough. The ribbon bends always toward the same direction because the side with the

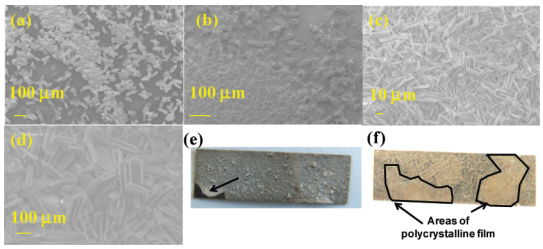

Figure 3. SEM images of the (a,b) concave and (c,d) convex side of the metglas ribbon. Photographs of the (e) convex and (f) concave side of the ribbon. The arrow on panel (e) points to an area where the film has been peeled off and the arrows on panel (f) point to the "islands" of polycrystalline films.

continuous film always faces down. The effect of adsorption induced strains is more pronounced on continuous films because of the absence of free space between the crystals that can accommodate the strains. The above suggest that the bending in Figure 1 is a result of the expansion of the bottom film and that the stains are tensile. The most striking observation (Figure 3 c, d) is the absence of any SEM detectable cracks on the convex side of the film. Even though the formation of nanometer sized cracks can not be excluded, this finding clearly indicates that it should be possible to form continuous zeolite films with high elasticity even at large and repetitive strains without loss of film connectivity due to crack formation. The films have been tested numerous times in a duration of couple of years without peeling from the metglas surface, indicating the good affinity between the two layers.

The conditions used for the synthesis of the silicalite-1 films are similar to those used in the past for the preparation of silicalite-1 membranes on stainless steel supports which exhibited n-C_4H_{10}/i-C_4H_{10} ideal permselectivity ~5.4 at 200 °C.[28] Despite this fact, it is not clear whether the film shown in Figure 3 would have had permselective performance if it was grown on a porous substrate. It is possible, however, to estimate the stresses and strains of the metglas ribbon and the silicalite-1 film from the ribbon's radius of curvature using the standard beam theory.[31] For each vapor, the radius of a circle that fits the sensor's curvature is shown in Table 1. According to the theory, inside a bent beam there is always a stress-free plane along the beam, known as "the neutral plane" and the strains are measured with respect to it. The strain on a point located at a distance y from the neutral plane is equal to the ratio y/R where R is the ribbon curvature (see the Supporting Information). We calculated the strain at the external surface of the zeolite film assuming that the neutral plane is at the concave surface of the ribbon. As shown in Table 1, the adsorption induced strains decrease in the following order of organic vapors: *n*-hexane, *p*-xylene, *o*-xylene, benzene, and *c*-hexane. Adsorption induced strains are usually estimated from analyzing X-ray or neutron diffraction patterns.[16,32−35] Our data are in fairly good agreement with these values (Table 1). Even though we measure strains only along the ribbon's axis, the silicalite-1 film has no preferred orientation and thus the observed strain represents some sort of an average strain in all crystallographic directions. However, in general, film flexibility is expected to depend on crystal orientation. Note that for the *c*-hexane/silicalite-1 case there are no crystallographic data available, at least to the best of our knowledge. On the other hand, it is generally accepted[32,35] that c-hexane does not transform the silicalite-1 lattice from monoclinic to orthorombic providing a possible explanation for the very small strain. For the case of benzene our data agree well with the results of B.F. Mentzen[33] but

Table 1. Radius of Curvature and Corresponding Strains of the Silicalite-1/Metglas Ribbon Due to Adsorption of Organic Vapors and Comparison with Literature Data[a]

			unit-cell parameter change reported in the literature (%)			
organic vapor	radius of curvature (cm)	strain (%)	*a*	*b*	*c*	ref
air	4.58	0.0				
n-hexane	1.17	3.82	2.49	5.37	4.1	16
c-hexane	4.24	0.11				
benzene	2.55	1.04	−1.3	0.9	0.4	16
			0.65	0.76	1.12	33
o-xylene	2.05	1.52				
p-xylene	1.76	1.62	0.97	2.27	5.3	34

[a] The strains shown are relative to equilibration in air.

not with those of Sorenson et al.[16] The reason for this discrepancy is not currently known. Even though crystallographic data for the system *o*-xylene/silicalite-1 are available in the literature,[36,37] it is not possible to compare them with our data because the authors did not report the data for the empty crystals.

In conclusion, the elasticity and flexibility of the silicalite-1 film due to the adsorption of organic vapors is demonstrated. The corresponding strains are different for each organic vapor and they are visible with naked eye. These results can provide an insight into the design of zeolite permselective membrane materials, or toward understanding the zeolite membrane performance. Furthermore, they indicate that zeolite films are ideal candidates for the design of novel zeolite film based applications, such as multifunctional composite sensors, or self-adjusting smart valves that will open or close depending on the gas concentration. Additional studies are currently in progress in order to (a) examine the effect of different concentrations on induced strain; (b) link the adsorption induced strain with permselective membrane performance; (c) study the effect of crystal orientation on the zeolite film flexibility; and (d) develop a methodology for obtaining quantitative information about the strain from the Metglas resonance frequency measurements.

■ ASSOCIATED CONTENT

Supporting Information. Video recording of adsorption induced strains on the silicalite-1/metglas ribbon 2 (AVI); experimental procedure (PDF). This material is available free of charge via the Internet at http://pubs.acs.org.

■ AUTHOR INFORMATION

Corresponding Author

*Fax: (+) 30-2610965223, E-mail: vnikolak@iceht.forth.gr.

■ ACKNOWLEDGMENT

We thank Dr V. Dracopoulos for the acquisition of the SEM images.

■ REFERENCES

(1) McLeary, E. E.; Jansen, J. C.; Kapteijn, F. *Microporous Mesoporous Mater.* **2006**, *90*, 198.
(2) Xu, X. W.; Wang, J.; Long, Y. C. *Sensors* **2006**, *6*, 1751–1764.
(3) Zijian, L.; Mark, C. J.; Minwei, S.; Ryan, E. T.; David, J. E.; Wolfgang, M.; Jeremy, I. M.; Shuang, L.; Christopher, M. L.; Junlan, W.; Michael, W. D.; Mark, E. D.; Yushan, Y. *Angew. Chem., Int. Ed.* **2006**, *45*, 6329–6332.
(4) Lew, C. M.; Cai, R.; Yan, Y. *Acc. Chem. Res.* **2010**, *43*, 210–219.
(5) Hashimoto, S.; Moon, H. R.; Yoon, K. B. *Microporous Mesoporous Mater.* **2007**, *101*, 10.
(6) Kim, H. S.; Sohn, K. W.; Jeon, Y.; Min, H.; Kim, D.; Yoon, K. B. *Adv. Mater.* **2007**, *19*, 260.
(7) Yoon, K. B. *Acc. Chem. Res.* **2007**, *40*, 29.
(8) Kuhn, J.; Motegh, M.; Gross, J.; Kapteijn, F. *Microporous Mesoporous Mater.* **2009**, *120*, 35.
(9) Kuhn, J.; Gascon, J.; Gross, J.; Kapteijn, F. *Microporous Mesoporous Mater.* **2009**, *120*, 12.
(10) Snyder, M. A.; Tsapatsis, M. *Angew. Chem., Int. Ed.* **2007**, *46*, 7560.
(11) Gounaris, C. E.; Wei, J.; Floudas, C. A.; Ranjan, R.; Tsapatsis, M. *AIChE J.* **2009**, *56*, 611.
(12) Choi, J.; Ghosh, S.; King, L.; Tsapatsis, M. *Adsorption* **2006**, *12*, 339.
(13) Nair, S.; Lai, Z.; Nikolakis, V.; Bonilla, G.; Tsapatsis, M. *Microporous Mesoporous Mater.* **2001**, *48*, 219–228.
(14) Nair, S.; Tsapatsis, M. . In *Handbook of Zeolite Science and Technology*; Auerbach, S. M., Karrado, K. A., Dutta, P. K., Eds.; Marcel Dekker: New York, 2003.
(15) Morell, H.; Angermund, K.; Lewis, A. R.; Brouwer, D. H.; Fyfe, C. A.; Gies, H. *Chem. Mater.* **2002**, *14*, 2192.
(16) Sorenson, S. G.; Smyth, J. R.; Kocirik, M.; Zikanova, A.; Noble, R. D.; Falconer, J. L. *Ind. Eng. Chem. Res.* **2008**, *47*, 9611.
(17) Sorenson, S. G.; Payzant, E. A.; Noble, R. D.; Falconer, J. L. *J. Membr. Sci.* **2010**, *357*, 98–104.
(18) Sorenson, S. G.; Smyth, J. R.; Noble, R. D.; Falconer, J. L. *Ind. Eng. Chem. Res.* **2009**, *48*, 10021.
(19) Lee, J. B.; Funke, H. H.; Noble, R. D.; Falconer, J. L. *J. Membr. Sci.* **2008**, *321*, 309–315.
(20) Yu, M.; Falconer, J. L.; Amundsen, T. J.; Hong, M.; Noble, R. D. *Adv. Mater.* **2007**, *19*, 3032.
(21) Xomeritakis, G.; Lai, Z.; Tsapatsis, M. *Ind. Eng. Chem. Res.* **2001**, *40*, 544–552.
(22) Lee, J. B.; Funke, H. H.; Noble, R. D.; Falconer, J. L. *J. Membr. Sci.* **2009**, *341*, 238–245.
(23) Giannakopoulos, I. G.; Kouzoudis, D.; Grimes, C. A.; Nikolakis, V. *Adv. Funct. Mater.* **2005**, *15*, 1165–1170.
(24) Baimpos, T.; Kouzoudis, D.; Nikolakis, V. *Sci. Adv. Mater.* **2010**, *2*, 1–4.
(25) Gora, L.; Kuhn, J.; Baimpos, T.; Nikolakis, V.; Kapteijn, F.; Serwicka, E. M. *Analyst* **2009**, *134*, 2118–2122.
(26) Squire, P. T. *J. Magn. Magn. Mater.* **1990**, *87*, 299–310.
(27) Livingston, J. D. *Phys. Status Solidi A* **1982**, *70*, 591–596.
(28) Tuan, V. A.; Li, S. G.; Falconer, J. L.; Noble, R. D. *J. Membr. Sci.* **2002**, *196*, 111–123.
(29) Baimpos, T.; Nikolakis, V.; Kouzoudis, D. *Stud. Surf. Sci. Catal.* **2008**, *174*, 665–668.
(30) Treacy, M. M. J.; Higgins, J. B.; von Ballmoos, A. *Zeolites* **1996**, *16*, 323–802.
(31) Nash, W. A., *Theory and Problems of Strength of Materials*, 4th ed.; McGraw-Hill: New York, 1998.
(32) Ashtekar, S.; Hastings, J. J.; Gladden, L. F. *J. Chem. Soc. Faraday Trans.* **1998**, *94*, 1157.
(33) Mentzen, B. F. *Mater. Res. Bull.* **1987**, *22*, 337.
(34) Mentzen, B. F.; Gelin, P. *Mater. Res. Bull.* **1999**, *30*, 373.
(35) Muller, J. A.; Conner, W. C. *J. Phys. Chem.* **1993**, *97*, 1451.
(36) Nair, S.; Tsapatsis, M. *J. Chem. Phys.* **2000**, *104*, 8982.
(37) Fyfe, C. A.; Lee, J. S. J.; Cranswick, L. M. D.; Swainson, I. *Microporous Mesoporous Mater.* **2008**, *112*, 299.